THE JOURNAL OF PHYSICAL CHEMISTRY Letters

Letter

pubs.acs.org/JPCL

Anomalous Hysteresis in Perovskite Solar Cells

Henry J. Snaith,* Antonio Abate, James M. Ball, Giles E. Eperon, Tomas Leijtens, Nakita K. Noel, Samuel D. Stranks, Jacob Tse-Wei Wang, Konrad Wojciechowski, and Wei Zhang

Department of Physics, University of Oxford, Clarendon Laboratory, Parks Road, Oxford OX1 3PU, United Kingdom

Supporting Information

ABSTRACT: Perovskite solar cells have rapidly risen to the forefront of emerging photovoltaic technologies, exhibiting rapidly rising efficiencies. This is likely to continue to rise, but in the development of these solar cells there are unusual characteristics that have arisen, specifically an anomalous hysteresis in the current−voltage curves. We identify this phenomenon and show some examples of factors that make the hysteresis more or less extreme. We also demonstrate stabilized power output under working conditions and suggest that this is a useful parameter to present, alongside the current-voltage scan derived power conversion efficiency. We hypothesize three possible origins of the effect and discuss its implications on device efficiency and future research directions. Understanding and resolving the hysteresis is essential for further progress and is likely to lead to a further step improvement in performance.

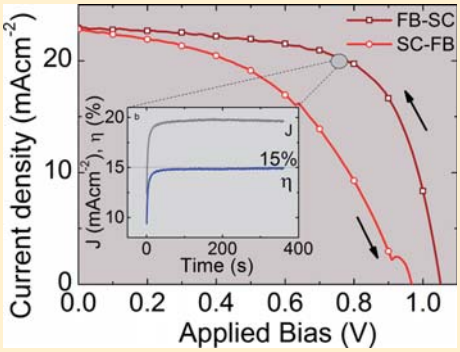

SECTION: Energy Conversion and Storage; Energy and Charge Transport

Perovskite solar cells have rapidly risen to the forefront of emerging photovoltaic technologies, exhibiting externally verified power conversion efficiencies of over 16%.[1−10] Device efficiencies are extracted from current−voltage (J−V) curves, which are usually measured by exposing a solar cell to a standardized light source (typically air mass (AM) 1.5, 100 mW cm^{-2} irradiance) and sweeping an applied bias across the terminals of the cell over a predetermined voltage range while measuring the current flowing in the external circuit. This is intended to closely represent the steady-state power output of a solar cell at any given bias and should not be dependent on bias sweep rate or sweep direction and not usually upon light exposure history. However, there are many instances when pre-exposure to light, typically termed light soaking, is employed to enhance the performance of both dye-sensitized[11−13] and organic solar cells.[14,15] For both of these technologies, the improvements (or changes under light soaking) are interpreted to be due to photoinduced doping or alterations of the electronic states on the surfaces of metal oxide layers employed. With respect to scan rate, electrolyte-based dye-sensitized solar cells have a very slow response time to an abrupt change in load, and care has to be taken not to scan the current-voltage curves too fast. Differences in the shape of the current-voltage curve, scanning from short-circuit to forward bias and back again, typically arise from the capacitance of the solar cell. If the scanning is done too fast, then the solar cell can charge up under forward bias conditions, and extra-capacitive charge, in addition to the photogenerated charge, can be extracted when the solar cell is swept rapidly to short circuit. When sweeping from short circuit to open circuit too quickly, the photogenerated charge can partially charge the solar cell, and the amount of charge flowing into the external circuit can be reduced as a consequence. These differences in the current measured in the forward and reverse scanning directions manifest as hysteresis in the current-voltage curves. Even for silicon solar cells, hysteresis in the current-voltage curves can occur if the bias is swept extremely fast, with complete scans performed in less than 2 to 44 ms depending on the precise cell architecture. This corresponds to a scan rate of 15 to 300 V/s, below which errors for capacitive effects are minimized.[16]

For perovskite solar cells measured under certain scanning conditions, significant hysteresis can be present in the current−voltage curves. However, unlike what would be expected from typical capacitive charging and discharging effects, the hysteresis often gets more extreme as the scan rate is reduced, and even at extremely slow scan rates there can still be significant hysteresis. To reach stabilized current output, the voltage step in some instances has to be held constant for hundreds of seconds, resulting in impractically slow scan rates required to determine a true "steady-state" current voltage curve. We show some examples of the impact that the perovskite solar-cell architectures and the scanning routines have upon hysteresis and discuss the possible origins and implications of these observations. This is not an exhaustive study but highlights a key area for future investigation.

We will discuss the three predominant perovskite solar-cell architectures in this letter: (i) planar heterojunction solar cells with no mesoporous oxide,[7,17] (ii) perovskite-sensitized solar cells fabricated on mesoporous TiO_2,[1,3] and (iii) meso-superstrutured solar cells (MSSCs) which employ mesoporous

Received: January 17, 2014
Accepted: March 24, 2014
Published: March 24, 2014

Al_2O_3 as an inert scaffold in place of the TiO_2.[4] The solar cells of this work are all fabricated with a mixed halide perovskite $CH_3NH_3PbI_{3-x}Cl_x$, as described in previous publications.[4,5] For a detailed description of the differences and operating principles of these device architectures, please see the referenced literature.[10]

Starting with solution-processed planar heterojunction solar cells,[17] if scanned at 0.3 V/s it is possible to measure current−voltage curves without significant hysteresis, as we show in Figure 1. These scans start and finish under forward bias.

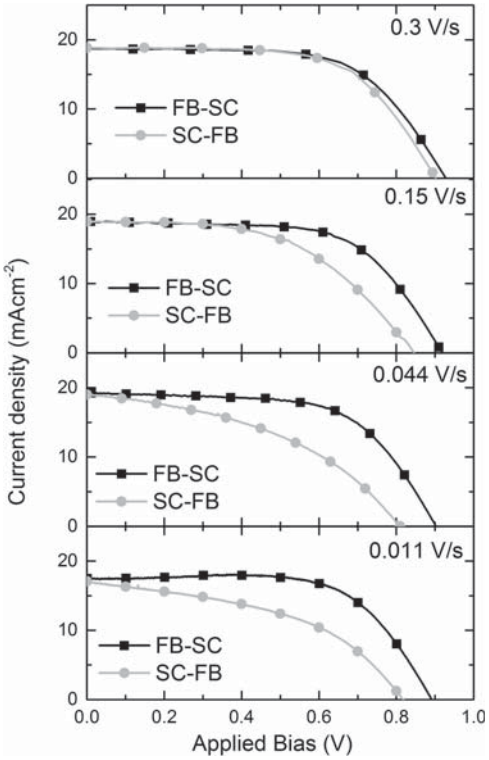

Figure 1. Influence of scanning conditions on planar heterojunction perovskite solar cell current−voltage characteristics. From forward bias to short circuit (FB-SC, black) and from short circuit to forward bias (SC-FB, gray) current density−voltage curves for a single-solution-processed planar heterojunction perovskite solar cell measured under simulated AM1.5 100 mW cm^{-2} sun light at a range of scan rates from 0.3 to 0.011 V/s. The scans start and finish under forward bias and have 60 s of stabilization time at forward bias (1.4 V) under illumination prior to scanning.

However, by slowing down the scan rate, hysteresis emerges, which progressively gets more and more severe as the scan rate is slowed from 0.3 to 0.011 V/s.

The previous trend is opposite to that reported by Dualeh et al., who observed that hysteresis in perovskite-sensitized TiO_2 solar cells becomes progressively less severe as the scan rate was slowed from 0.2 to 0.01 V/s.[18] In Figure 2, we show the current−voltage characteristics for mesoporous TiO_2-based perovskite solar cells with a range of mesoporous TiO_2 thicknesses. For the thickest mesoporous TiO_2 (750 nm), all of the perovskite has infiltrated the porous films, and these devices are likely to be operating as a sensitized solar cell,[1,3,4] where the perovskite absorbs the light and rapidly transfers its charge to the n-type TiO_2 and p-type hole-transporter. As the TiO_2 is thinned down to 260 nm, a solid-capping layer of

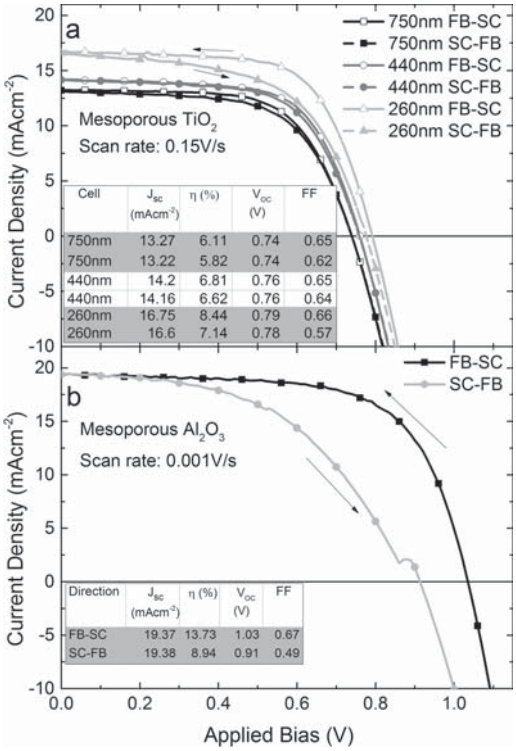

Figure 2. Influence of solar cell architecture upon current−voltage hysteresis. Forward bias to short circuit (FB-SC) and short circuit to forward bias (SC-FB) current−voltage curves measured under simulated AM1.5 100 mW cm^{-2} sun light for: (a) Mesoporous TiO_2-based perovskite solar cells, with 750, 440, and 260 nm thick mesoporous TiO_2, coated with 40 wt % perovskite solution, with a scan rate of 0.15 V/s, starting from FB and held for a 2 s stabilization time at FB (1.4 V) before the scan commences. For both the 750 and 440 nm thick TiO_2, all of the perovskite infiltrates the mesoporous TiO_2, and there is substantially no solid perovskite capping layer; for the 260 nm thick mesoporous TiO_2, there exists a ∼200 nm-thick solid perovskite capping layer. (b) Mesoporous alumina-based MSSC with a 400 nm thick mesoporous alumina film coated with a 40 wt % perovskite solution, scanned at 0.001 V/s starting from FB, and held for a 2s stabilization time under illumination before the scan commences. For the MSSC, the mesoporous alumina is infiltrated with perovskite, but in addition there exists a ∼300 nm thick solid perovskite capping layer. The table insets give the extracted solar-cell performance parameters. For each thickness in panel a, the first row is FB-SC and the second row is SC-FB.

perovskite is formed, and the photoactive layer of the device is composed of two strata, one operating as an inorganic bulk heterojunction between TiO_2 and perovskite and the top layer as a solid perovskite thin film.[19] Specific details of this device structure will be described elsewhere.[20] The hysteresis is relatively small for all of these devices, but it does increase measurably going from the thick to thin mesoporous TiO_2. As displayed in Figure S3 in the Supporting Information, such sensitized solar cells made in our laboratory also show the unexpected trend in hysteresis (at similar scan rates), opposite to those in the study by Dualeh et al.,[18] suggesting that the phenomenon is heavily dependent on architecture and processing conditions.

For mesosuperstructured solar cells (MSSCs), which are based on a mesoporous alumina scaffold with the presence of a solid perovskite capping layer, the hysteresis is also present and

dx.doi.org/10.1021/jz500113x | J. Phys. Chem. Lett. 2014, 5, 1511−1515

significantly more evident than for the cells employing mesoporous TiO_2. The example we show in Figure 2b is for an extremely slow scan rate of 0.001 V/s (dwell time of 10s per 10 mV step), where the hysteresis is rather pronounced. We show the scan rate dependence of such a cell in Figure S2 in the Supporting Information and for the MSSCs there is only a small change in the relative scale of the hysteresis with changing scan rate, with hysteresis again being slightly less at high scan rates. In addition, the overall determined power conversion efficiency is higher with the faster scan rates.

It is a rather unsatisfying situation that the determined efficiency is so strongly dependent on measuring protocol and apparent history, that even when scanned at impractically slow sweep rates, significant hysteresis can still persist for the perovskite solar cells. However, the current−voltage scan is simply intended to be a straightforward means to determine the steady-state maximum power output of the cell. Measuring the steady-state power output directly at a given forward bias is also a feasible means to estimate the power conversion efficiency. In Figure 3a, we show a current−voltage curve for a well-operating MSSC scanned at a sweep rate of 0.15 V/s starting from forward bias to short circuit and back from short circuit to forward bias. The maximum power point on the first scan (forward bias to short circuit) is 15.5 mW cm^{-2} (equivalent to 15.5% power conversion efficiency), whereas on the reverse scan it is only 10.2 mW cm^{-2}. In Figure 3b, we show that the transient photocurrent rises with the solar cell being slowly scanned (total scan time 500 s) from 0.75 to 0.74 V and back again, for the same MSSC, which was measured rapidly in Figure 3a. The power output approaches 15 mW cm^{-2} over the 500s measurement window, which gives reasonable confidence that the forward bias to short circuit scan gives a close estimate for the "steady-state" efficiency. However, clearly comparing both the current-voltage curves and stabilized power output gives a more complete picture of the operation of the solar cell. We therefore propose that for as long as the hysteresis persists the stabilized power output near the maximum power point should be presented, along with the current−voltage curves, identifying scan rate and direction. In the Supporting Information (Figures S1 and S4), we also show similar measurements for planar heterojunction and perovskite-sensitized solar cells, respectively. Both of these cell architectures show a drop in stabilized power output in comparison with the FB-SC scan, but the drop is most extreme for the planar heterojunction devices. Comparison of the stabilized power output is clearly important when understanding how new adaptations have impacted upon the cells performance. Using this as a figure of merit will also direct the research toward optimization of the technology toward high stabilized power-conversion efficiency rather than maximizing the peak point on the $J-V$ curve. We also note that the same steady-state photocurrent and power-conversion efficiency are achieved regardless of the "history" of the solar cell; there is no difference in the maximum power-point-stabilized photocurrent if the cell was held at forward bias or at short circuit just prior to the measurement, as shown in Figure S5 in the Supporting Information. The steady state is, however, reached over several minutes at the maximum power point. While the hysteresis should then be decreased upon scanning at even slower rates than the slowest rate attempted in this study of 0.01 V s^{-1}, this is extremely impractical. Therefore, to summarize, it appears that the hysteresis is not present at extremely fast scan rates (0.3 V s^{-1}), gets worse as the scan rate is slowed to 0.01 V s^{-1}, and again reduces at impractically slow scan rates ($\ll$0.01 V s^{-1}). The implications are discussed later.

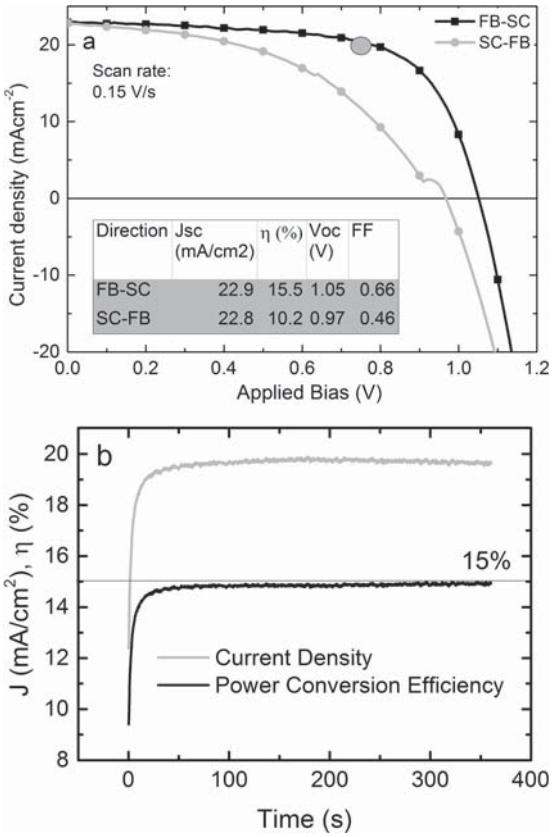

Figure 3. Stabilized power output from an MSSC. (a) Forward bias to short circuit (FB-SC) and short circuit to forward bias (SC-FB) current−voltage curves measured under AM1.5 simulated sun light for a MSSC fabricated with a 400 nm thick mesoporous alumina film coated with a 40 wt % perovskite solution. The inset table gives the FB-SC- and SC-FB-determined performance parameters. (b) Photocurrent density and power conversion efficiency as a function of time for the same cell held close to 0.75 V forward bias. The cell was in the dark under open-circuit prior to the start of the measurement. The large gray circle on panel a is the stabilized power output after 500 s of illumination under load.

Before we can proceed to understand or even speculate upon the origin of the hysteresis, we need to determine whether it arises from the perovskite layer, the p- or n-type collection materials (spiro-OMeTAD or TiO_2, respectively), or the interface between the perovskite and the charge collection contacts. As a first level of interrogation, we have fabricated perovskite-based MSSCs with no compact TiO_2 (fluorine-doped tin oxide (FTO) only as the electron collection layer), and with no spiro-OMeTAD (Au only as the hole collection layer). For both of these cell architectures, the hysteresis is extremely severe. This strongly suggests that the hysteresis is not specifically caused by the compact TiO_2 nor the hole-transporter and is hence a property of the perovskite absorber or the interface between the perovskite and the charge-collection layers. The increased severity of the hysteresis in both of these configurations (Au-only and FTO-only) suggests that it is influenced by the contact materials and it may originate from an interface effect rather than a bulk property of

dx.doi.org/10.1021/jz500113x | J. Phys. Chem. Lett. 2014, 5, 1511−1515

the perovskite layer. Considering both the behavior with FTO-only and that with the flat and mesoporous TiO_2, it is consistent that a contact resistance for electron transfer between the perovskite and TiO_2 is at the root of the hysteresis. Considering such, the mesoporous TiO_2 would offer a lower contact resistance for forward electron transfer from the perovskite due to the higher surface area, reducing the severity of the phenomenon. Recombination of electrons in the perovskite with the Au electrode is likely to be faster than with holes in the spiro-OMeTAD, hence exaggerating the impact of slow electron collection for the device with no hole-transporter.

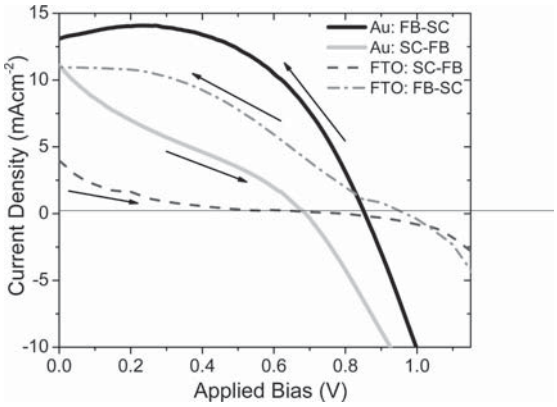

Figure 4. Impact of p- and n-type charge collection layers on hysteresis. Forward bias to short circuit (FB-SC) and short circuit to forward bias (SC-FB) current−voltage curves measured under simulated AM1.5 100 mW cm^{-2} sun light for perovskite MSSCs with either no Spiro-OMeTAD (Au only) or no compact TiO_2 (FTO only). The scan rate was 0.1 V/s.

Summarizing all of the previous data, the main observations are that: (1) The hysteresis predominantly arises from the presence of the perovskite absorber in the solar cell. (2) The hysteresis is strongly dependent on the contact material, including p- and n-type contacts, and mesoporous versus planar heterojunctions. (3) The rise time to reach stabilized power output is very slow, on the order of 100 s. (4) Slowing down the scan rate generally increases rather than reduces the degree of hysteresis for planar heterojunction solar cells within a given range of scan rates, but ultimately steady state is reached at any applied bias irrespective of history.

Our interpretation of these observations is that the characteristics are likely to arise due to a change to the nature of the electronic contact between the perovskite and the p- and n-type contact materials, but we emphasize that this interpretation should be subject to further scrutiny. We see three possible origins which may be uniquely responsible or all contributing to the effect:

(i) The perovskite absorbers may have a very large defect density within or near the surface of the material or specifically generated interface states.[21] These defects could act as traps for electrons and holes and fill under forward bias working conditions, resulting in good p- and n-type contacts at the interfaces. Under short-circuit conditions, the traps may empty due to charge transfer directly to the p- and n-type contacts, resulting in poor operation until the traps are filled once more. The slow emptying and filling of traps would be consistent with a slow component in the current and voltage decay, which has been observed by Dualeh et al. In the case of no p- or n-type blocking layers, traps may empty more rapidly upon moving toward short-circuit due to increased recombination at the unblocked contacts, resulting in more significant hysteresis. In addition, accelerated recombination with opposite carriers at the heterojunctions between the perovskite and the metallic electrodes may exaggerate the issue of contact resistance at the opposite electrode. If this is the relevant mechanism, it is likely that the lack of hysteresis at very high scan rates (after holding the cell at forward bias) is simply because the emptying of traps toward short circuit occurs at a slower rate than the scan rate. This would be consistent with the identical steady-state performances (Figure S5 in the Supporting Information) for cells held at different biases prior to the maximum power point measurement. The trapping and detrapping times are likely to vary with architecture and processing, explaining the different time scales for different device architectures and certainly across different laboratories.

(ii) The organometal trihalide perovskites have been observed to possess ferroelectric properties, and a slow polarization of the material may occur, which will be dependent upon applied bias.[22] This polarization could have a number of influences, including making charge collection more or less favorable at the contacts. However, careful interrogation of the relative frequency of the ferroelectric switching needs to be performed to establish if it is feasibly responsible for the hysteresis.

(iii) Excess ions, as interstitial defects (iodide or methylammonium) may be present and predominantly labile throughout the film. Under operation the interstitial ions would be able to migrate to either side of the film, which could advantageously screen space charge buildup, aiding charge collection under working conditions.

Key parameters to discriminate between the possible origins are likely to be determined by investigating the transient, temperature and light intensity dependence, the current−voltage curves, and other optoelectronic measurements, coupled to detailed theoretical modeling. Alongside, a trial and error approach to resolve the issue through intuitive material substitution and optimization is also likely to prove fruitful.

In summary, we have demonstrated that there is often an anomalous hysteresis present in the current−voltage characteristics of perovskite solar cells and that the specific device architecture is influential to the severity of the effect. We have demonstrated that even with the presence of hysteresis, the stabilized power output under applied bias at the maximum power point can approach that determined by the fast current−voltage sweep from forward bias to short-circuit, but this is not always the case. We therefore suggest that both the stabilized power output near the maximum power point and the current voltage curves are presented and compared, for as long as the hysteresis persists. We have proposed three possible origins but highlight now that extensive investigation is required to understand and resolve this phenomenon. Although stabilized power output is possible under working conditions with the current technology, the peculiar current−voltage characteristics are likely to make maximum power point tracking under variable illumination conditions more challenging than with well-behaved solar cells. The anomalous hysteresis is therefore a central challenge to resolve for further rapid progress and adoption of perovskite photovoltaics. It is also likely that a

dx.doi.org/10.1021/jz500113x | J. Phys. Chem. Lett. 2014, 5, 1511−1515

solution to this peculiar artifact will also result in a step increase in performance, specifically in device fill factor.

■ ASSOCIATED CONTENT

Supporting Information

Device fabrication and solar cell characterization details. Current−voltage characteristics. Scan rate dependence of the current−voltage characteristics of a mesosuperstructured perovskite solar cell and perovskite-sensitized solar cell. Current−voltage characteristics of a perovskite-sensitized solar cell. Extracted current density from a planar perovskite cell over time, when the cell is held at different voltage conditions until stabilized. This material is available free of charge via the Internet at http://pubs.acs.org.

■ AUTHOR INFORMATION

Corresponding Author

*E-mail: h.snaith1@physics.ox.ac.uk.

Notes

The authors declare no competing financial interest.

■ ACKNOWLEDGMENTS

This work was supported by EPSRC and the European Research Council (ERC) through the HYPER PROJECT no. 279881. G.E.E. is supported by the EPSRC and Oxford Photovoltaics Ltd. through a Nanotechnology KTN CASE award. J.T.-W.W. is supported by Swire Educational Trust. T.L. is supported by the European Union Seventh Framework Program [FP7/2007-2013] under Grant Agreement 316494.

■ REFERENCES

(1) Kojima, A.; Teshima, K.; Shirai, Y.; Miyasaka, T. Organometal Halide Perovskites as Visible-Light Sensitizers for Photovoltaic Cells*J. Am. Chem. Soc.* **2009**, *131*, (17), 6050.

(2) Im, J. H.; Lee, C. R.; Lee, J. W.; Park, S. W.; Park, N. G. 6.5% Efficient Perovskite Quantum-Dot-Sensitized Solar Cell . *Nanoscale* **2011**, *3* (10), 4088−4093.

(3) Kim, H. S.; Lee, C. R.; Im, J. H.; Lee, K. B.; Moehl, T.; Marchioro, A.; Moon, S. J.; Humphry-Baker, R.; Yum, J. H.; Moser, J. E.; Gratzel, M.; Park, N. G. Lead Iodide Perovskite Sensitized All-Solid-State Submicron Thin Film Mesoscopic Solar Cell with Efficiency Exceeding 9%. *Sci. Rep.* **2012**, 2.

(4) Lee, M. M.; Teuscher, J.; Miyasaka, T.; Murakami, T. N.; Snaith, H. J. Efficient Hybrid Solar Cells Based on Meso-Superstructured Organometal Halide Perovskites. *Science* **2012**, *338* (6107), 643−647.

(5) Ball, J. M.; Lee, M. M.; Hey, A.; Snaith, H. J. Low-Temperature Processed Meso-Superstructured to Thin-Film Perovskite Solar Cells. *Energy Environ. Sci.* **2013**, *6* (6), 1739−1743.

(6) Burschka, J.; Pellet, N.; Moon, S.-J.; Humphry-Baker, R.; Gao, P.; Nazeeruddin, M. K.; Gratzel, M. Sequential Deposition As a Route to High-Performance Perovskite-Sensitized Solar Cells. *Nature* **2013**, *499* (7458), 316−319.

(7) Liu, M.; Johnston, M. B.; Snaith, H. J. Efficient Planar Heterojunction Perovskite Solar Cells by Vapour Deposition. *Nature* **2013**, *501* (7467), 395−398.

(8) Noh, J. H.; Im, S. H.; Heo, J. H.; Mandal, T. N.; Seok, S. I. Chemical Management for Colorful, Efficient, and Stable Inorganic−Organic Hybrid Nanostructured Solar Cells. *Nano Lett.* **2013**, *13* (4), 1764−1769.

(9) Park, N.-G. Organometal Perovskite Light Absorbers Toward a 20% Efficiency Low-Cost Solid-State Mesoscopic Solar Cell. *J. Phys. Chem. Lett.* **2013**, *4* (15), 2423−2429.

(10) Snaith, H. J. Perovskites: The Emergence of a New Era for Low-Cost, High-Efficiency Solar Cells. *J. Phys. Chem. Lett.* **2013**, *4* (21), 3623−3630.

(11) Tiwana, P.; Docampo, P.; Johnston, M. B.; Herz, L. M.; Snaith, H. J. The Origin of an Efficiency Improving "Light Soaking" Effect in SnO_2 Based Solid-State Dye-Sensitized Solar Cells. *Energy Environ. Sci.* **2012**, *5* (11), 9566−9573.

(12) Yang, L.; Xu, B.; Bi, D.; Tian, H.; Boschloo, G.; Sun, L.; Hagfeldt, A.; Johansson, E. M. J. Initial Light Soaking Treatment Enables Hole Transport Material to Outperform Spiro-OMeTAD in Solid-State Dye-Sensitized Solar Cells. *J. Am. Chem. Soc.* **2013**, *135* (19), 7378−7385.

(13) O'Regan, B.; Schwartz, D. T. Large Enhancement in Photocurrent Efficiency Caused by UV Illumination of the Dye-Sensitized Heterojunction TiO_2/RuLL'NCS/CuSCN: Initiation and Potential Mechanisms. *Chem. Mater.* **1998**, *10* (6), 1501−1509.

(14) Gilot, J.; Wienk, M. M.; Janssen, R. A. J. Double and Triple Junction Polymer Solar Cells Processed from Solution. *Appl. Phys. Lett.* **2007**, *90*, 143512.

(15) Sista, S.; Park, M.-H.; Hong, Z.; Wu, Y.; Hou, J.; Kwan, W. L.; Li, G.; Yang, Y. Highly Efficient Tandem Polymer Photovoltaic Cells. *Adv. Mater.* **2010**, *22* (3), 380−383.

(16) Herman, M.; Jankovec, M.; Topič, M. Optimal *I*−*V* Curve Scan Time of Solar Cells and Modules in Light of Irradiance Level. *Int. J. Photoenergy* **2012**, *2012*, 151452-1−151452-11.

(17) Eperon, G. E.; Burlakov, V. M.; Docampo, P.; Goriely, A.; Snaith, H. J. Morphological Control for High Performance, Solution-Processed Planar Heterojunction Perovskite Solar Cells. *Adv. Funct. Mater.* **2014**, *24* (1), 151−157.

(18) Dualeh, A.; Moehl, T.; Tétreault, N.; Teuscher, J.; Gao, P.; Nazeeruddin, M. K.; Grätzel, M. Impedance Spectroscopic Analysis of Lead Iodide Perovskite-Sensitized Solid-State Solar Cells. *ACS Nano* **2013**, *8* (1), 362−373.

(19) Heo, J. H.; Im, S. H.; Noh, J. H.; Mandal, T. N.; Lim, C.-S.; Chang, J. A.; Lee, Y. H.; Kim, H.-j.; Sarkar, A.; Nazeeruddin, Md. K.; Gratzel, M.; Seok, S. I. High-Performance Inorganic-Organic Hybrid Heterojunction Solar Cells. *Nat. Photon.* **2013**, *7* (6), 486−491.

(20) Leijtens, T.; Lauber, B.; Eperon, G. E.; Stranks, S. D.; Snaith, H. J. The Importance of Perovskite Pore Filling in Organometal Mixed Halide Sensitized TiO_2-Based Solar Cells. *J. Phys. Chem. Lett.* **2014**, *5*, 1096−1102.

(21) Kim, H.-S.; Mora-Sero, I.; Gonzalez-Pedro, V.; Fabregat-Santiago, F.; Juarez-Perez, E. J.; Park, N.-G.; Bisquert, J. Mechanism of Carrier Accumulation in Perovskite Thin-Absorber Solar Cells. *Nat. Commun.* **2013**, *4*, 2242.

(22) Stoumpos, C. C.; Malliakas, C. D.; Kanatzidis, M. G. Semiconducting Tin and Lead Iodide Perovskites with Organic Cations: Phase Transitions, High Mobilities, and Near-Infrared Photoluminescent Properties. *Inorg. Chem.* **2013**, *52* (15), 9019−9038.